Thermal and Air Permeation Properties of a Carbon Fiber/Toughened Epoxy Based Prepreg System

SANG-BEOM SHIM,[1] JAMES C. SEFERIS[2]

[1] Laboratory for Manufacturing and Productivity, Department of Mechanical Engineering, Bldg. 35-234, Massachusetts Institute of Technology, Cambridge, Massachusetts 02139

[2] Polymeric Composites Laboratory, Department of Chemical Engineering, University of Washington, Seattle, Washington 98195

Received 11 September 1996; accepted 1 November 1996

ABSTRACT: This study addresses thermal and air permeation properties of a new toughened prepreg system. Voids in the uncured prepreg structure can affect the void content in the final composite structure. A new, toughened prepreg system, commercially available for aircraft structural application, was utilized in this study. The prepreg was subjected to thermal and rheological characterization to understand the basic prepreg properties. These experiments were followed by a prepreg air permeation study to investigate prepreg processing and its influence on the prepreg structure. Crosslinking of the resin matrix was monitored with prepreg specimens without extracting resin from the prepreg. Along with thermal property measurements, the air flow rate significantly decreased in initial static experiments, followed by equilibrium permeability values. An air permeation model divided the air permeability into intralaminar and interlaminar permeabilities. Interlaminar air permeation was found to be more pronounced than intralaminar air permeation in this particular prepreg system. These permeation measurement results were explained using optical microscopy, proving that the application of vacuum could eliminate significant porosity in the laminate. Collectively, understanding prepreg thermal and air permeation properties was considered to be important; the voids in uncured prepreg may cause the voids in the final composite structure. Voids in the prepreg can be attributed to the heterogeneity and anisotropy of the toughened prepreg structure, resulting from particular prepreg processing techniques.
 J Appl Polym Sci **65:** 5–16, 1997

Key words: prepreg; air permeation; crosslinking; porosity; impregnation

INTRODUCTION

Over the past several decades, composite materials, especially fiber-reinforced plastics, have been utilized increasingly to replace traditional airplane structural materials, such as metals. Composites made of high-performance prepregs (fibers preimpregnated with resin) have drawn much attention from the aircraft industry and have been well utilized among all composite materials. This has stimulated a variety of advanced technologies to improve the quality of composites. Because of ease of use and extensive experience, autoclaving with prepreg layup is presently the most prevalent technology in the manufacturing of high-performance composites. In spite of this progress, prepreg processing has been considered more of an art than a science, where continuous fibers are impregnated with resin by trial and error. Although the airplane industry has several decades

Correspondence to: J. C. Seferis.
Contract grant sponsor: Heath Tecna Aerospace Company.

of trial-and-error experience, the philosophical viewpoints of prepreg processing are not yet substantiated or controlled by an adequate scientific approach.

Thermoset composites are known to have damage tolerance inferior to that of thermoplastic composites. The modification of resin by rubber or thermoplastic toughening agents may be able to enhance the damage tolerance. Some toughened systems rely on the inherent high toughness of toughening agents; others use phase separation, creating a plastic deformation zone with heterogeneous toughening domains. Although it is proven that the toughening agents increase the damage tolerance of thermoset composites, the incorporation of these toughening agents into the base resin system also increases the resin viscosity, causing difficulty with resin impregnation during the hot-melt impregnation process. A final link between the toughened prepreg system and a viscous modified resin is achieved by "lacquered film impregnation," a combination of solvent impregnation and hot-melt impregnation technologies. This lacquered film impregnation process enables the development of toughened prepreg systems with high melt viscosity. As the importance of this toughened prepreg system becomes more pronounced, the understanding of prepreg properties is gaining more attention, encouraging further investigation of the relation of the prepreg processing conditions to the thermal properties of prepreg systems.

While the prepreg thermal properties are related to the resin properties, porosity in prepreg structures results from the prepreg processing conditions. Voids in composite structures are one of the concerns that need to be efficiently controlled during fabrication. As many researchers have mentioned, voids in composites are regarded as detrimental to the composite structure's achieving adequate performance during airplane service life.[1] By changing the manufacturing process, voids can be eliminated or even created in composite structure. These manufacturing process parameters include pressure, resin viscosity, temperature, textile geometry,[2] permeability, and resin curing behavior. These parameters can influence the void content in composite structures separately or synergetically.

The permeability in prepreg systems is stated by researchers to be an important parameter which indicates the porosity of prepreg structures. Depending on the prepreg processing conditions, the porosity is influenced by the microstructure and can be evaluated by air-permeation measurements. Nam and colleagues[3] developed air permeation equipment which could be installed in autoclave environments. Their experiments utilized a high-performance prepreg system currently used for honeycomb processing. Their equipment was able to measure the air flow changes during autoclave heating conditions as well as at room temperature. Ahn and coworkers[4] utilized similar equipment and developed air permeation models to separate the contribution between intra- and interlaminar air permeation. These results provided insight into how prepregs are structured and influenced by prepreg processing. Air permeation research was further conducted to investigate the prepreg permeability changes upon aging time and fiber orientation.[5] As aging time increased beyond a certain period, prepreg permeability significantly increased, which was attributed to the loss of prepreg tack. As new, toughened prepreg systems and their processing techniques are being developed, the new, toughened prepreg microstructure remains to be elucidated for the understanding of new prepreg system and processing modifications. The permeability measurements are supposed to be a versatile methodology to meet these objectives.

Accordingly, this study focused on establishing a basis of the process–structure–property relationships regarding voids in the unidirectional, new, toughened prepreg system. Thermal and rheological characterization methodology was applied to monitor crosslinking of the toughened prepreg system and the processing influences on the cure-reaction mechanism. Extensive utilization of air-permeation equipment is addressed in this study. These results were accompanied by optical microscopic study to enhance the scientific knowledge of prepreg microstructure and the porosity distribution.

EXPERIMENTAL

Prepreg Characterization

A carbon-fiber unidirectional tape system impregnated with a toughened epoxy resin was used as a model prepreg system to achieve a better understanding of process-induced voids in unidirectional carbon/epoxy composites, along with inherent characteristics in the prepreg system. High-performance Ciba Fibredux 924C/T-300S-34 unidirectional tape, qualified as BAER 3212 by the British Aerospace

Company (Filton, UK) was utilized as the prepreg system. This prepreg consisted of Toray T-300-600 carbon fiber and 34 ± 2.5 wt % of toughened epoxy.[6,7] Thermal and rheological analyses of the prepreg were conducted to obtain information concerning prepreg processability. Heat of reaction was measured using a TA Instruments Differential Scanning Calorimetry (DSC) 910 model and analyzed by a TA Instruments Thermal Analyzer 2000 system. Samples weighing 10 mg were sealed in aluminum pans heated to 370°C at a heating rate of 5°C/min. Total heat of reaction was obtained from the area above the baseline consistent with eq. (1)[8]:

$$\Delta H = \int_{T_i}^{T_f} \left(\frac{dH}{dT} \right) dT \qquad (1)$$

where ΔH is the total heat of reaction; T_i is initial reaction temperature; and T_f is the final reaction temperature.

The degree of cure was measured by DSC, ramping to 330°C after the simulated autoclave cure cycle. The simulated cure cycle included ramping to cure temperature of 177°C at a 2.5°C/min heating rate, isothermal heating at 177°C for 2 h, followed by cooling to room temperature.

Weight loss of uncured prepregs generated during processing was measured by a Hi-Res Thermal Gravimetric Analyzer (TGA) 2950. The TGA samples weighed approximately 25 mg and were heated to 177°C with a 2.5°C/min heating rate, followed by a 2-h simulated autoclave cure cycle at 177°C (350°F) isothermal cure temperature.

A Rheometrics RMS 601 was used to evaluate the viscosity change that took place during the autoclave process. Since the epoxy resin of the prepreg system was not available, a sample consisting of eight cross-plied prepregs was mounted between 25-mm-diameter parallel plates and heated to 177°C at a 2.5°C/min heating rate, followed by a 177°C isothermal hold until the prepreg specimen was hardened. An initial frequency of 10 Hz and initial strain of 10% were applied to conduct the viscosity measurements. The physical interpretation of the prepreg viscosity is a combination of fiber friction and resin viscosity change, which is different from a regular neat-resin viscosity change during the cure process, but this information could indicate when gelation took place.

Utilizing these experiments, information regarding physicochemical and chemorheological prepreg properties was obtained for the further characterization of prepreg impregnation and cure mechanisms.

Air Permeation and Optical Microscopy of Uncured Prepreg

Air-permeation measurement is a tool to define the prepreg degree of impregnation which may govern composite properties such as void content and its distribution. Many experiments have been conducted on the air-permeation behavior attributed to prepreg porosity and fiber arrangements.[9] For this study, a recently developed prepreg airflow measurement device was installed in an autoclave (Lipton). The dimension of the device was approximately 30 × 30 cm (1 × 1 ft). As Figure 1 indicates, the configuration of the sample mounting was similar to the autoclave layup procedure. One or four plies of prepreg specimens of 5 × 8 cm were laid up longitudinally to the air flow direction. After the prepreg layup, the airflow measurement device was installed to the autoclave, followed by vacuum application. The air flow was measured by a flow meter and recorded for 30 min, when an equilibrium condition was reached. This static air-flow measurement was followed by dynamic air-flow measurements by varying the vacuum pressure to 0 in Hg and then back to the full vacuum condition. This time, both the air flow and vacuum pressure values were recorded.

This air-flow experiment was designed for understanding the prepreg porosity, which could be related to the prepreg microscopic structure. Therefore, optical microscopy was used to investigate the porosity of the fresh prepreg system. This optical microscopic study started from a special sample preparation with fresh prepreg, polished for clarity. Special polishing skill was necessary because the fresh prepreg was very soft at room temperature, which caused much more difficulty than cured composite polishing techniques. After the sample polishing, a Nikon Optiphot-Pol Optical microscope was utilized to investigate the porosity locations in the prepreg system. Both one- and five-plied unidirectional prepreg specimens were utilized to investigate the porosity of the prepreg structure.

RESULTS AND DISCUSSION

Understanding prepreg systems and their void-formation mechanisms is important in composite

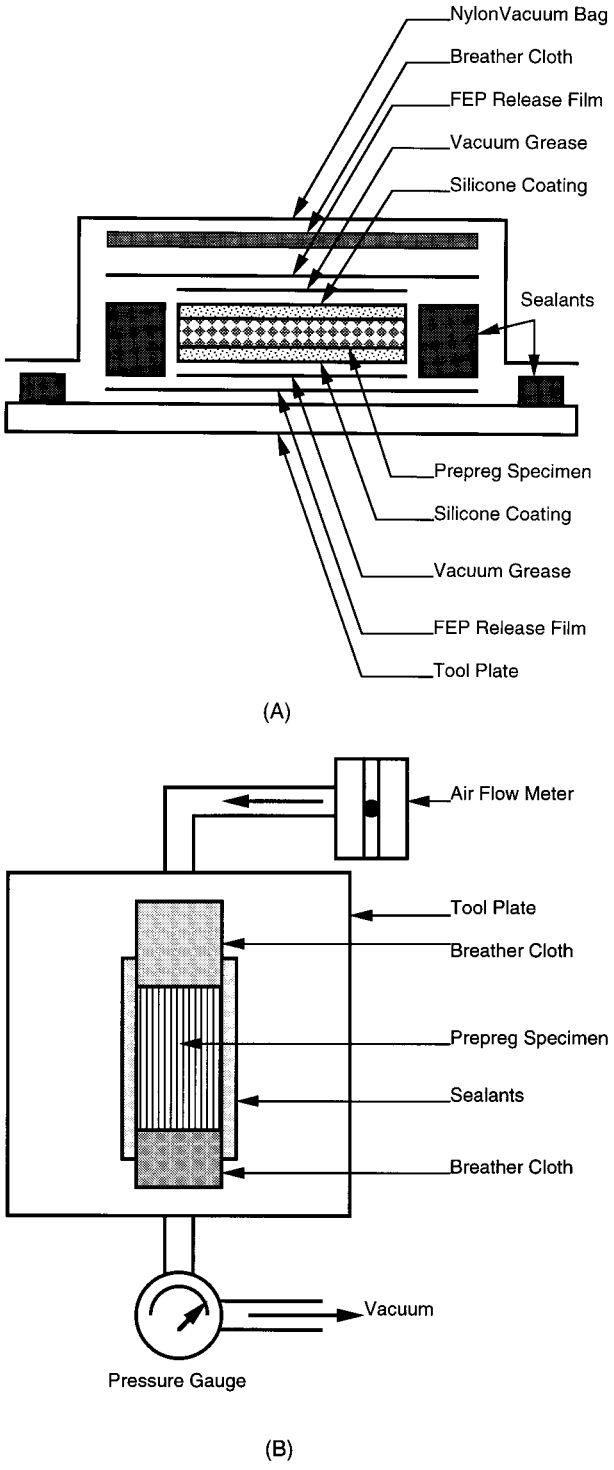

Figure 1 Schematic description of air-flow measurement device installed in autoclave: (A) cross section of sample mounting; (B) top view of the installation.

lamination processing because prepreg physical and chemorheological properties can influence the impregnation and cure behavior during autoclave processing, and because the voids can be generated by these inherent prepreg properties.[10] In addition, voids generated by the inherent prepreg properties can degrade composite performance. Therefore, this research incorporated these aforementioned concepts into an evaluation for prepreg thermal and gas permeation properties. The results of this investigation allowed us to conclude that the prepreg porosity could be characterized by air-permeation measurements and that this air permeation property was viscoelastic, attributed to a heterogeneous and anisotropic structure in a new, toughened prepreg system. Accordingly, properties, processing, and structure in composites were correlated and these principles provided the understanding of air permeation phenomena in this unidirectional prepreg system.

Prepreg Characterization

Results of dynamic DSC experiments are shown in Figure 2 for both (A) unreacted and (B) 2-h isothermally cured Fibredux 924C/T-300S-34 prepreg systems used in this study. The thermogram shown in Figure 2(A) indicates that there are two exotherms which may be attributed to different crosslinking reactions. Based on other resin characterization results, the first exotherm may be due to major resin–hardener reaction, while the higher exotherm could represent homopolymerization. With a total heat of reaction of 203 J/g, the lower exotherm appeared to dominate the autoclave cure process at 177°C (350°F). After the simulated autoclave cure cycle, Figure 2(B) shows that the first exotherm disappeared, leaving the higher-temperature exotherm. The residual heat of reaction was 31.7 J/g with a 0.84 degree of cure.

Prepregs with a minimum of volatiles or low-molecular-weight components would be promising materials for a variety of high-performance applications in engineering design because the resulting composite would have a reduced void content. The TGA thermogram in Figure 3 showed that some volatiles evolved during the 177°C 2-h isothermal cure cycle, thus high autoclave pressure would be required to suppress volatilization. This volatile component may be attributed to low-molecular-weight components of resin or residual solvents left during prepregging processes, but the weight losses of the prepreg were reasonable for composite fabrication.

The prepreg viscosity profile exhibited crosslinking during the 2-h isothermal heating. Figure

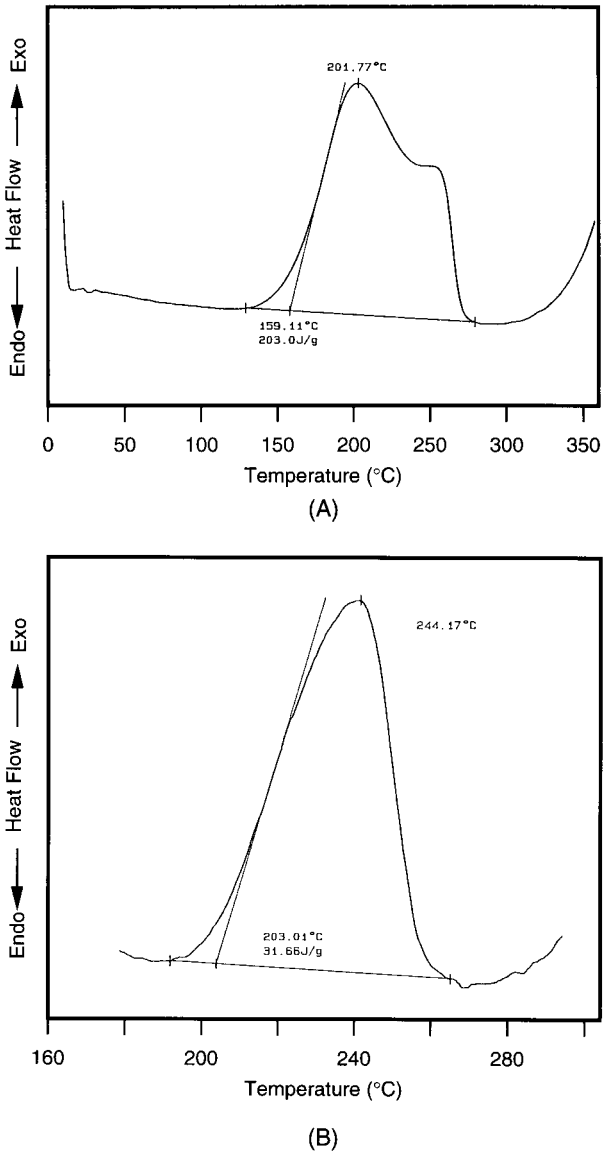

Figure 2 DSC thermograms of Fibredux 924C/T-300S-34 unidirectional prepreg system, performed with a 5°C/min heating rate: (A) uncured; (B) after 2-h isothermal curing at 177°C.

4 is the viscosity profile of Fibredux 924C/T-300S-34 cross-plied unidirectional prepreg system. In fact, this viscosity profile does not describe pure resin viscosity change, but exhibits the combination of resin viscosity and fiber friction between plies. At the initial stage, the prepreg surface was covered with resin and the inside of the prepreg was partially impregnated, containing porosity. Therefore the viscosity value was most influenced by resin viscosity decrease, corresponding with initial decrease during the initial heating stage. After a certain heating temperature ($\approx$70°C) the

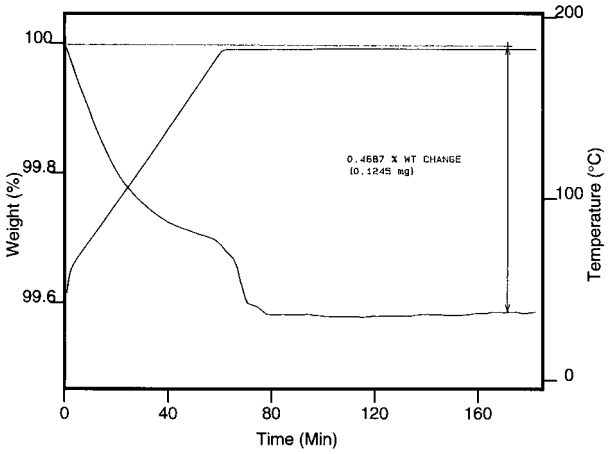

Figure 3 TGA thermogram of Fibredux 924C/T-300S-34 unidirectional prepreg system performed with a simulated autoclave process.

resin gained enough viscosity to infuse the fibrous preform, and some resin was squeezed out of the compressed sample. The resin impregnation into the prepreg resulted in an increase in the influence of the fiber surface friction on the viscosity value at the minimum resin viscosity range. Since resin did not give any satisfactory resistance to oscillatory input, the viscosity value was controlled by fiber friction until the crosslinking began at the initial isothermal cure stage, when gelled resin viscosity increased enough to respond to oscillatory inputs. This resin crosslinking was indicated by the steep increase in viscosity. Therefore the viscosity profile of prepreg was a combination of resin chemorheology and fiber friction.

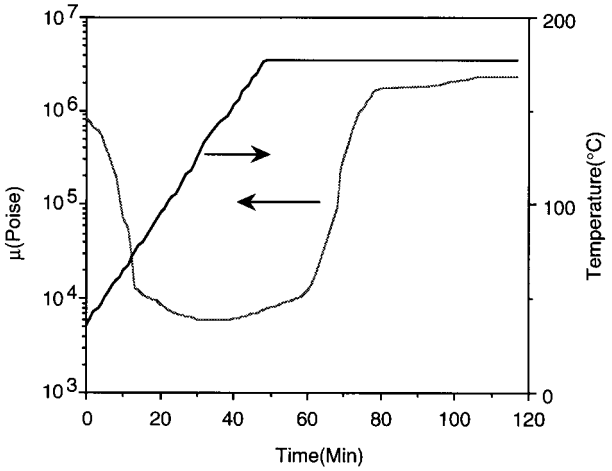

Figure 4 Viscosity profile of Fibredux 924C/T-300S-34 cross-plied unidirectional prepreg system performed with a RMS 601 rheometer.

Collectively, the basic prepreg properties discussed in this section could provide information on how to design autoclave cure processes. This information was also considered to be related to the other information which will be discussed later. More study regarding the prepreg viscosity is needed in the future.

Air-Permeation Study

Air permeation measurement is a tool used to define the prepreg degree of impregnation that can be used to grade the prepreg properties. The air-permeation apparatus utilized in this work was recently developed to be compatible with the autoclave. The principal advantage of this autoclave-installed air-permeation equipment was that the autoclave pressure influence on the prepreg consolidation process could be observed through the pressure and temperature application. Along with the experimental equipment development, the theoretical background was established from the Ahn–Seferis air permeation model[4,9] and the well-known Darcy's law as follows:

$$Q = -\frac{KA_p}{\mu}\frac{dP}{dx} \tag{2}$$

where Q is the volumetric air flow rate through the prepreg laminate (cm^3/s); A_p is the cross-sectional area of the prepreg laminate (cm^2); K is the overall transverse air permeability of the prepreg laminate (cm^2); μ is the viscosity of the air (Pa s); and $\frac{dP}{dx}$ is the pressure gradient in the prepreg open space, which the original Ahn–Seferis air permeation model assumed to have linear pressure differences as

$$\frac{dP}{dx} = \frac{P_a - P_V}{L_p} \tag{3}$$

where P_a is the atmospheric pressure (Pa); P_V is the pressure in the vacuum bag (Pa); and L_p is the length of the prepreg laminate (cm).

For the modification, this new air-permeation study used an ideal gas law assumption:

$$PQ = \dot{n}RT = C\ (\text{const}) \tag{4}$$

where $\dot{n}$ is the molar air flow rate (mol/s); R is the gas constant (8.314 J/Kmol); and T is the absolute temperature of the air (K).

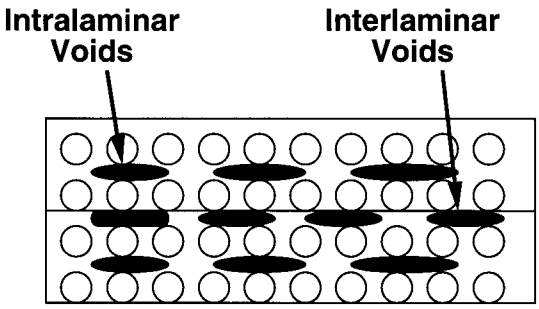

Figure 5 Schematic description of prepreg laminates showing interlaminar and intralaminar air permeation mechanisms.

This assumption was integrated into Darcy's law; that is to say,

$$\frac{C}{P} = -\frac{KA_p}{\mu}\frac{dP}{dx} \tag{5}$$

$$\int_0^{L_P} C\,dx = -\int_{P_a}^{P_V}\frac{A_P K}{\mu}P\,dP \tag{6}$$

$$CL_P = -\frac{A_P K}{2\mu}(P_V^2 - P_a^2) \tag{7}$$

$$C = \frac{A_P K}{2\mu L_P}(P_a^2 - P_V^2) \tag{8}$$

At atmospheric pressure,

$$P_a Q_a = C = \frac{A_P K}{2\mu L_P}(P_a^2 - P_V^2) \tag{9}$$

$$Q_a = \frac{A_P K}{2\mu L_P}\left(P_a - \frac{P_V^2}{P_a}\right) = \frac{KA_P\Delta P}{2\mu L_P} \tag{10}$$

where $\Delta P = P_a - (P_V^2/P_2)$. Therefore, the $\Delta P - Q_a$ curves for prepreg systems are fairly linear, and permeability K can be obtained from eq. (10).

The most significant advantage of this study was that the air permeability could be divided into two subsequent permeabilities: intralaminar and interlaminar. These two different permeabilities were caused by the intralaminar and interlaminar porosity, as shown in Figure 5. The measured overall permeability (K) was a combination of interlaminar permeability (K_i) and intralaminar permeability (K_b). Intralaminar voids exhibited a fiber directional-dependent distribution caused by the prepregging process, especially for unidirectional prepregs. Therefore K_b could be expressed as a tensor quantity depending on the fiber orien-

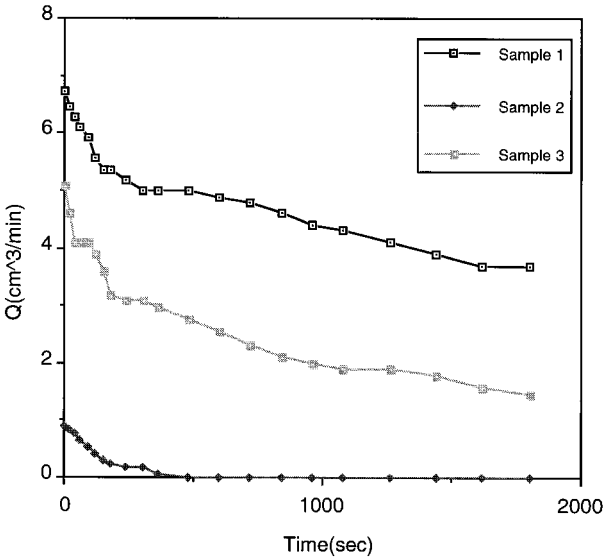

Figure 6 Volumetric air-flow rate of one-layered Fibredux 924C/T-300S-34 prepreg as a function of elapsed time.

tation as well as the fiber type. K_i also depended on the direction and should be described as a tensor even though the anisotropic effect was much more diminished than for the intralaminar permeability.

In the case of a prepreg laminate composed of n_p layers, the number of inter- and intralaminar regions were $n_p - 1$ and n_p, respectively. Therefore the overall permeability could be expressed as

$$hK = n_p(h_bK_b) + (n_p - 1)(h_iK_i) \qquad (11)$$

where n_p is the number of prepreg plies used in the experiment; h_b is the intralaminar thickness (cm); h_i is the interlaminar thickness (cm); K_b is the intralaminar permeability (cm^2); and K_i is the interlaminar permeability (cm^2).

Ahn suggested the use of a combined value of the thickness and the permeability (h_bK_b and h_iK_i) which was proportional to the volumetric air flow rate through the prepreg laminate.[9] Therefore, more than two series of experiments with different number of plies could yield h_bK_b and h_iK_i, respectively.

Figure 6 is a time–air flow rate profile of one-layered prepreg specimens. As Figure 6 indicates, the volumetric air flow rate values are different among the specimens, indicating that the degree of impregnation was not consistent for each position in the prepreg products. This could be verified by optical microscopy, which is discussed at the end of this section. Initially, the air flow rate was drastically reduced, followed by an equilibrium. Sample 2 showed zero volumetric air flow rate, which may be attributable to the closure of open intralaminar voids during the vacuum application. Based on eq. (9), the overall permeability was calculated and is plotted in Figure 7. From Figure 7, K was calculated from eq. (10), with a constant prepreg cross-section area assumption. The overall permeability followed behavior similar to that observed in air flow-rate results in Figure 6, and equilibrium overall permeabilities showed scattering in their values. Therefore, from a process control viewpoint, more consistency in the air permeability will be necessary to further improve product quality in relation to reductions in the variations by a statistical control method such as the capacity index (Cpk) approach.[11]

While the static air-permeation measurements focused on equilibrium air flow rate, dynamic air-permeation measurements placed emphasis on the history of pressure-versus-airflow rate relationship. Figure 8 shows dynamic air permeation results for one-layer Fibredux 924C/T-300S-34 prepreg specimens. These experiments were performed after the 30-min static air permeation tests, whose results are plotted in Figure 6 and 7. Since one of the samples, sample 2, showed zero air flow after 30 min, only two specimens were tested with these measurements. Regardless of the absolute airflow rate, the pressure difference–airflow rate relationship showed a hysterisis of the prepreg air permeation behavior. While the

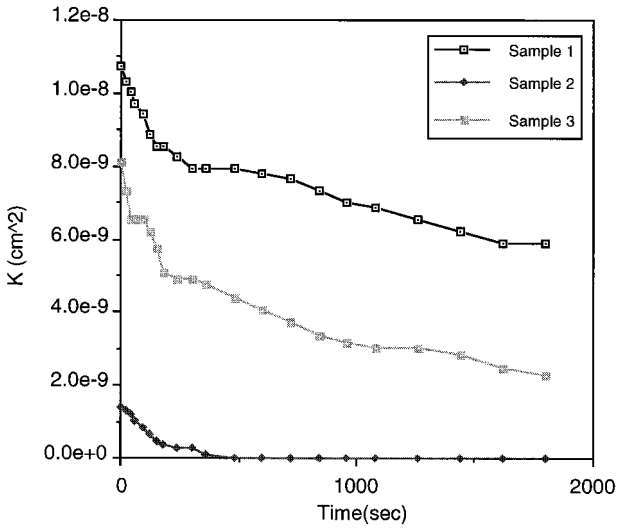

Figure 7 Permeability changes of one-layered Fibredux 924C/T-300S-34 prepreg specimens.

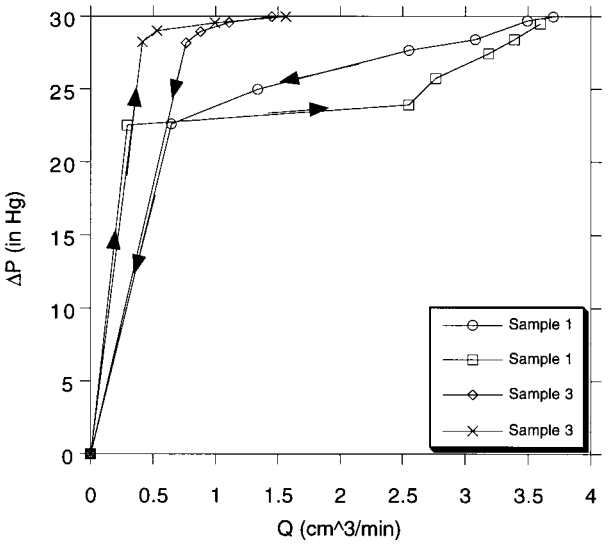

Figure 8 Dynamic air permeation measurement results of one-layered Fibredux 924C/T-300S-34 prepreg specimens.

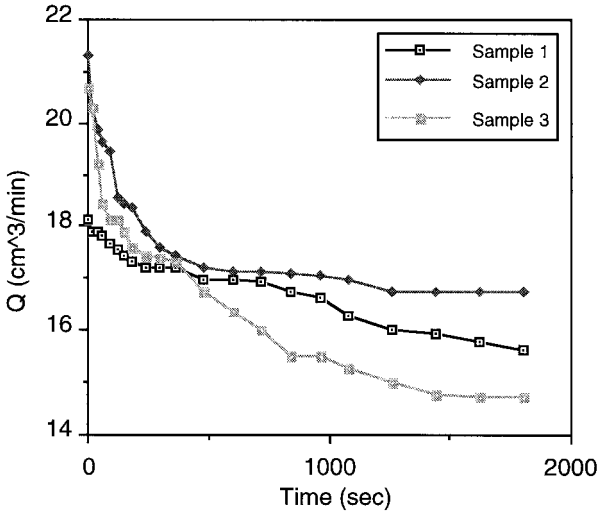

Figure 9 Volumetric air-flow rate of four-layered Fibredux 924C/T-300S-34 prepreg laminates.

air flow rate decreased as a function of the vacuum pressure difference ΔP, defined in eq. (10), the airflow rate increased sharply as the ΔP increased, approaching the original air flow rate. This hysterisis in the vacuum pressure-versus-airflow rate relationship may be attributed to the irreversible closure of open intralaminar voids. When the prepreg was released by the decrease in vacuum pressure, the air flow also decreased. However, if the vacuum pressure or ΔP increased, the previously open intralaminar voids were blocked by tacky resin, becoming partially closed intralaminar voids. In addition, fiber rearrangement that is different from previous fiber alignment would contribute to the air-permeation hysterisis. This hysterisis would disappear for dry fibers where only elasticity dominated in the system.

The static and dynamic air-permeation measurements were also performed for a four-layered prepreg to understand the air-permeation behavior change in laminates. Figure 9 presents the static air flow rate change of the four-layered laminates as a function of time. Contrary to the air flow rate of a single-layer prepreg, four-layered prepreg laminates exhibited a consistent-equilibrium air flow rate in all experiments. This consistency was attributed to averaging effects resulting from the stacking of several prepregs. Therefore it could be concluded that overall air flow rate was consistent and the overall air flow rate could explain processing effects on the average prepreg property. Calculated by eq. (9), the permeability–time relationship was presented as an alternative to the airflow rate–time relationship. Figure 10 represents the consistent permeability for three four-layered prepreg laminates. From the permeability results obtained in Figures 7 and 10, the overall permeability could be separated into the contributions from the intra-(K_b) and interlaminar (K_i) permeabilities. Again, eq. (11) was used with an averaged overall permeability of both single and four-layer laminates. The prepreg thickness was obtained from the prepreg specification as 1.22×10^{-2} cm.[6]

Table I summarizes the static air permeation

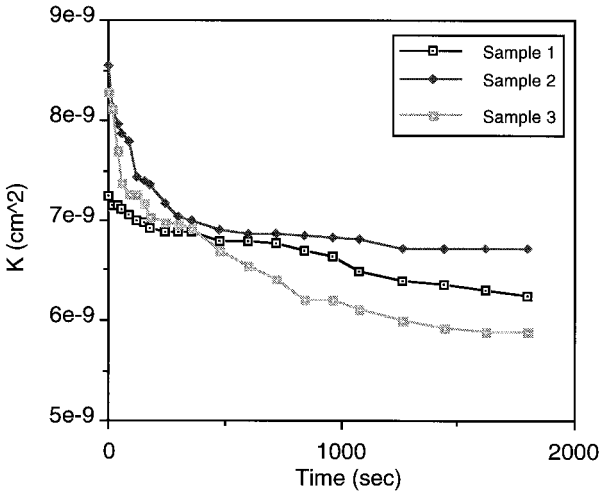

Figure 10 Permeability change of four-layered Fibredux 924C/T-300S-34 prepreg laminates.

Table I Air Permeation Measurement Results for Unidirectional Fibredux 924C/T-300S-34 Prepreg System

Permeation	Result
Intralaminar Permeation, h_bK_b $(cm)^3$	3.34×10^{-11}
Interlaminar Permeation, h_iK_i $(cm)^3$	5.76×10^{-11}
Relative Interlaminar Permeation, $[(h_iK_i)/(h_iK_i + h_bK_b)] \times 100$ (%)	63
Relative Intralaminar Permeation, $[(h_bK_b)/(h_iK_i + h_bK_b)] \times 100$ (%)	37

measurement results, showing that the interlaminar region occupied 63% of the open air path, but a significant proportion of the intralaminar region also contributed to air permeation. The combination of both inter- and intralaminar open air paths might be able to provide vacuum channels during vacuum-bag processes, reducing consequent void formation in composites.

The dynamic air permeation measurements of four-layered prepreg laminates indicate that the ΔP–Q graph followed the same path when the ΔP was reduced and increased. As Figure 11 presents, dynamic ΔP–Q behavior was insensitive to variations in the sample. In addition, the hysterisis observed in Figure 8 for the one-layered prepreg almost disappeared in the four-layered prepreg. The interlaminar region, which did not exist in the one-layered prepreg air permeation test, may have eliminated the hysterisis in this prepreg air permeation behavior, as is discussed later.

These air permeation measurements provide an understanding of the microscopic structure of the prepreg system, and how well the prepreg was impregnated with resin. With the objective of supplementing the versatility of the air permeation results, an optical microscopic study was also conducted. Figure 12 is a micrograph of Fibredux 924C/T-300S-34 prepreg surface magnified 100 times. As the figure shows, the prepreg surface (at left in Fig. 12) is partially covered by resin. Therefore, inconsistent air permeation results obtained for one-layered prepreg were found to result from irregular microscopic resin content in the prepreg. This irregular resin coverage was usually found in other prepreg systems, but this irregularity should be reduced for better quality control (high *Cpk*). As the number of prepreg layers increased in the laminates, this irregular resin coverage was eliminated due to averaging effects. In prepreg that was polished in a direction perpendicular to the fiber orientation, the intralaminar voids could be observed as a black, hollow space (Fig. 13). Also, the uncured resin mixed with a toughening agent was observed as cloudy valleys. In general, the black, hollow, intralaminar voids were distributed in a random manner caused by irregular impregnation in the prepreg. Therefore, we concluded that the irregular air permeation results for one-layered prepreg were due to the irregular void distribution. As the number of prepreg plies increased, the air permeation results become consistent.

The microscopic study mentioned above focused on one-ply prepreg. To understand the void distribution in laminates, five plies of uncured prepreg were laminated with a conventional layup procedure, followed by an optical microscopic study. Figure 14 is a micrograph of a five-layered uncured prepreg laminate cross section prepared by a standard layup procedure. From Figure 14, those black, hollow, intralaminar voids could be distinguished from resin impregnated area. These intralaminar voids were created by partial impregnation during the prepregging process, may inhibit the void-free composite fabrication, and should be eliminated for better performance. However, these large intralaminar voids might also be able to provide an open air channel so that vacuum is better applied inside laminates, eliminating air pockets entrapped during the prepreg layup procedure. The interlaminar voids did not seem to occupy a large area in this figure, but the intralaminar voids located next to the interlaminar voids created large inter/intralaminar voids in the laminate cross section. As the results obtained from air permeation measurements demonstrate, the intralaminar voids also contributed to overall permeability as well as interlaminar voids. Therefore, Figure 14 demonstrates that the results obtained from the air-permeation study are consistent with prepreg microstructural information.

Contrary to Figure 14, Figure 15 shows a reduced extent of intralaminar voids after a vacuum precompaction. Precompaction melds two sepa-

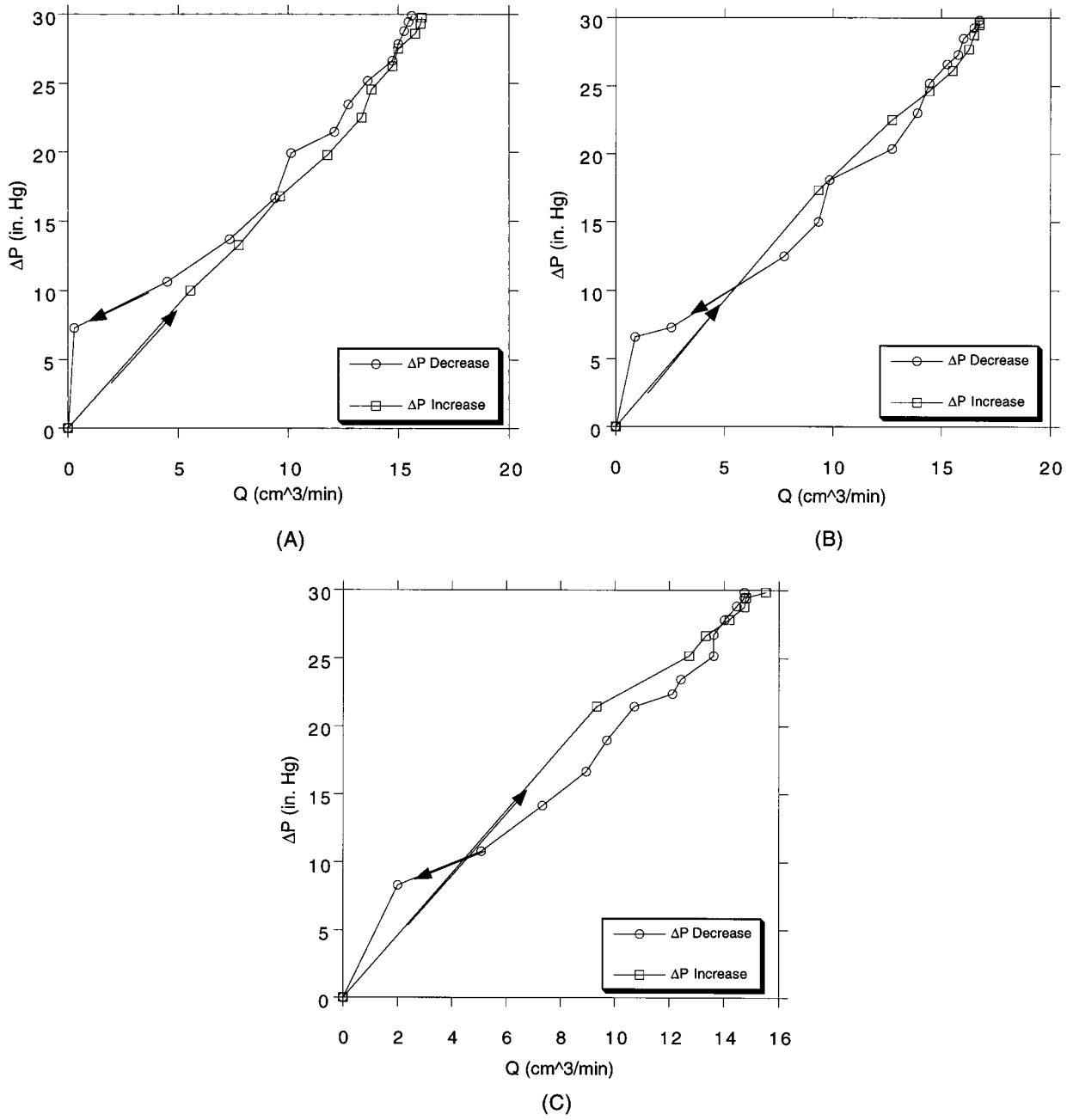

Figure 11 Dynamic air permeation measurement results of four-layered Fibredux 924C/T-300S-34 prepreg laminates: (A) sample 1; (B) sample 2; (C) sample 3.

rated intralaminar layers into one consolidated layer, reducing intralaminar void size. Even though precompaction could not eliminate all intralaminar voids, as the left center of Figure 15 indicates, the significant reduction in intralaminar void size could result in reduced void contents. However, the transformation from open air path into closed air entrapment might create voids during the autoclave processes. From Figure 15, small, round air pockets located in the interlaminar region may not be eliminated because of air entrapment during the layup.[12]

Collectively, air permeation measurement was shown to be a valuable prepreg characterization methodology that could correlate with prepreg microstructure and degree of impregnation. Distribution of intra- and interlaminar voids, along with the discussion about prepreg quality control,

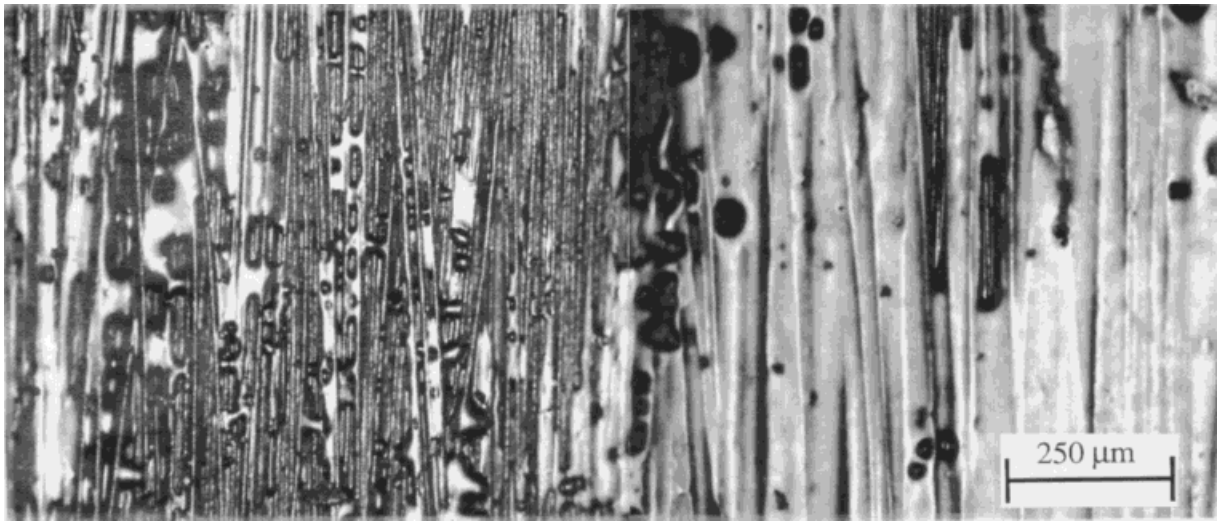

Figure 12 Micrograph of Fibredux 924C/T-300S-34 prepreg surface (100×).

was successfully evaluated. This integration of microscopic analysis and air-permeation measurements would be helpful in providing better methodology of controlling composite performance.

CONCLUSION

Thermal and gas permeation properties of a new, toughened prepreg system for high-performance aircraft structural composites were investigated to establish a process–structure–property relationship regarding void formation and its limitation on the composite application. The prepreg examined was a unidirectional carbon fiber/toughened epoxy system, toughened for better damage resistance. Thermal and rheological characterization of prepreg system was conducted for the purpose of investigating crosslinking reaction during a simulated autoclave process. This thermal characterization was accompanied by prepreg air-permeation study to better understand prepreg porosity as well as the "process-related" prepreg structure.

Thermal and rheological measurements of a prepreg system could monitor the crosslinking which was manifested in increased resin viscosity.

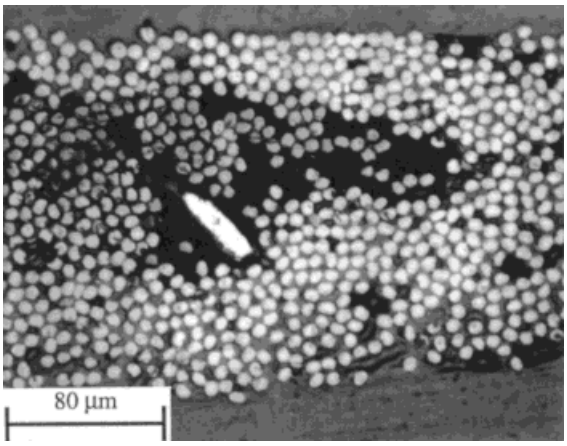

Figure 13 Micrographs of Fibredux 924C/T-300S-34 prepreg cross sections (400×).

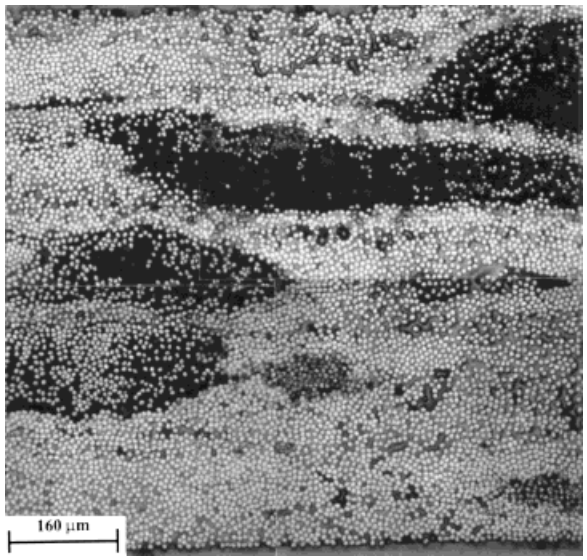

Figure 14 Micrograph of five-layered Fibredux 924C/T-300S-34 prepreg laminate cross section prepared with a standard layup procedure (200×).

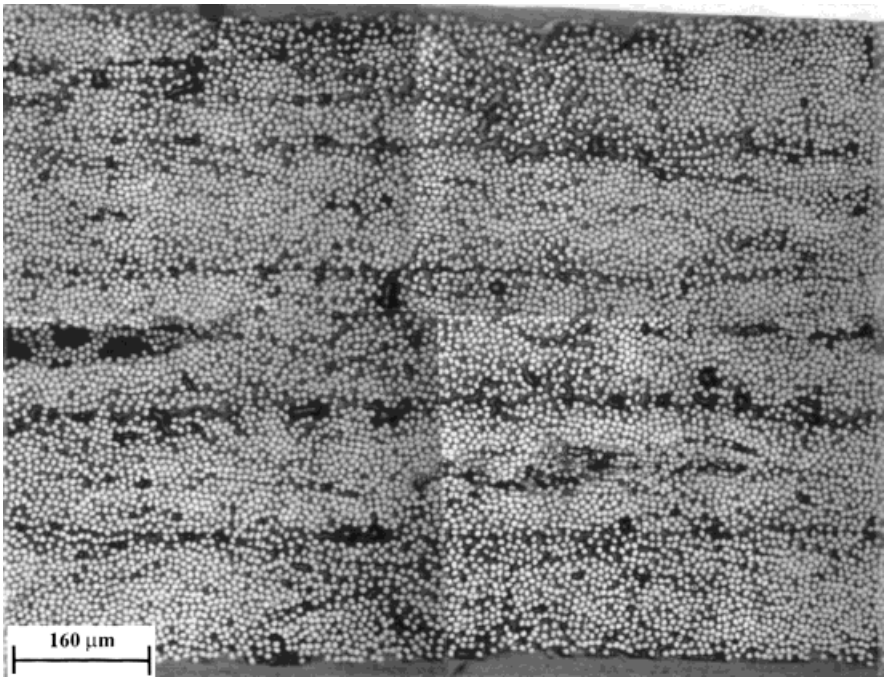

Figure 15 Micrograph of five-layered Fibredux 924C/T-300S-34 prepreg laminate cross section prepared with a full vacuum precompaction (200×).

Along with thermal characterization, air permeation measurements determined that the interlaminar permeability appeared to be more important than intralaminar permeability when the prepreg was laminated, creating an open air channel so that applied vacuum could reach further into a part. The contributions of interlaminar and intralaminar permeabilities were proved by optical microscopy. In addition, air permeation hysterisis was observed in this particular prepreg system.

This series of theoretical and experimental discussions provides an understanding of establishing manufacturing design criteria to optimize the prepreg porosity through gas permeation investigation. The porosity in prepreg was found to be attributed to partial impregnation; therefore, the requirements of the prepreg and controlled porosity reduction through the process modification were recommended for an appropriate process–structure–property relationship discussed in this study.

The authors express their appreciation to Mr. William Hudson and Mr. Keane Barthenheier of Heath Tecna Co. for their interest in and support of this research. Technical assistance of Ms. Lisa Ip is greatly appreciated. Financial assistance and material support for this research were provided by Heath Tecna Aerospace Company through project support to the Polymeric Composites Laboratory of the University of Washington.

REFERENCES

1. S.-B. Shim, K. J. Ahn, J. C. Seferis, A. J. Berg, and W. Hudson, *Polym. Composites,* **15**(6), 453 (1994).
2. S.-B. Shim, K. J. Ahn, and J. C. Seferis, *Proc. 6th. Tech. Conf. in Am. Soc. Comp.,* **6,** 1137 (1991).
3. J.-D. Nam, J. C. Seferis, S.-W. Kim, and K.-J. Lee, *Polym. Composites,* to appear.
4. K. J. Ahn, J. C. Seferis, J. O. Price, and A. J. Berg, *SAMPE J.,* **27**(6), 19 (1991).
5. J. W. Putnam and J. C. Seferis, *J. Adv. Mater.,* **26**(3), 35 (1995).
6. British Aerospace Company, BAER 3212 Specification, 1989.
7. Ciba Composites, Technical Communication, 1995.
8. R. B. Prime, in *Thermal Characterization of Polymeric Materials,* E. A. Turi, ed., Academic Press, New York, 1981, Chap 5.
9. K. J. Ahn, Ph.D. dissertation, University of Washington, 1990.
10. T. G. Gutowski, *SAMPE Quarterly,* **16**(4), 58 (1985).
11. A. G. Miller, D. T. Lovell, and J. C. Seferis, *Composite Structures,* **27**(1-2), 193 (1994).
12. J. M. Kenny, *Composite Structures,* **27,** 129 (1994).